Supporting Information

Sustainable and reusable electrospun g-C_3N_5/MIL-101(Fe)/poly(acrylonitrile-co-maleic acid) nanofiber for photocatalytic degradation of carbamazepine

Dongying Zhu,[a,b‡] Zhujun Huang,[a,b‡] Haiyan Wang,[b] Qiujun Lu,[b] Guihua Ruan,[a] Chenxi Zhao,[b] Fuyou Du[a, b*]

[a]Guangxi Key Laboratory of Electrochemical and Magnetochemical Functional Materials, College of Chemistry and Bioengineering, Guilin University of Technology, Guilin 541004, China

[b]College of Biological and Environmental Engineering, Changsha University, Changsha 410022, China

[‡]Dongying Zhu and Zhujun Huang contributed equally to this work.

Text S1

Characteristics of materials

The microstructure and surface morphology of materials were tested by scanning electron microscope (SEM, Hitachi SU8000, Japan) and transmission electron microscope (TEM, Tecnai G2 F30, PEI, USA), respectively. The elemental mappings and chemical compositions of the composites were performed by an energy-dispersive X-ray spectrometer (EDX) equipped on SEM. The surface area, pore volume and size of the photocatalysts were estimated by Micromeritics TriStar II 3020 analyzer (TriStar II 3020, Micromeritics Instrument Corporation, USA). The crystal phases of the composites were measured by X-ray diffraction (XRD, Brucker D8 Advance, Germany) with a Cu K_α radiation. The patterns of X-ray photoelectron spectroscopy were measured on a K-Alpha spectrometer (XPS, Thermo escalab 250Xi, Thermo Scientific, USA). TheThe chemical bonds analysis was investigated by the Nicolet Nexus 470 FT-IR spectrometer (Thermo Electron Corporation, USA). The active species to degrade carbamazepine were detected through trapping by BQ, t-BuOH, and EDTA-2Na (see Text S2). The characteristic signals of hydroxyl radicals (•OH) and superoxide anion radicals ($\bullet O_2^-$) were identified by electron spin resonance (ESR, Bruker A300-10/12, Germany), respectively. Photocatalytic degradation tests were carried out at room temperature under visible light irradiation (300W Xe lamp, CEL-HXF300, Aulight Co. Ltd., China) that equipped with a 380 nm cut-off filter ($\lambda > 380$ nm).

Text S2

Trapping experiments of active species

To probe the active species in degradation process, different scavengers (0.4 mmol) were added in sample solution besides E-spun g-C_3N_5/MIL-101(Fe)/PANCMA (20 mg), deionized water (20 mL) and carbamazepine solution (20 mL, 40 mg/L). Here benzoquinone (BQ, 0.5 mmol/L), tertiary butanol (t-BuOH, 5.0 mmol/L), and ethylene diamine tetraacetic acid disodium salt (EDTA-2Na, 1.0 mmol/L) were chosen as radical scavengers to capture superoxide radicals ($\bullet O_2^-$), hydroxyl radicals (•OH), and holes (h^+), respectively.

Text S3

LC-UV-MS analysis

UltiMate 3000 UHPLC (Thermo Fisher Scientific, USA), equipped with the Zorbax Eclipse Plus C18 column (4.6×250 mm, 5 μm), was used to detect the residual carbamazepine in sample solution. The possible intermediates of carbamazepine during the degradation process were identified by LC-MS (Q Exactive Focus MS, Thermo Scientific, USA).

For LC analysis, the mobile phase was composed of water (A, 60%) and acetonitrile (B, 40%) at a flow rate of 0.2 mL/min. The volume was 5 μL. The detection wavelength was 285 nm, and the column temperature was 30 °C. The typical LC chromatograms are shown in Fig. S2, and the obtained calibration curve was presented in Table S2.

For MS analysis, the MS analysis parameters were operated in the range of 50-500 m/z with a positive ion mode using ESI ion source. The sheath gas, aux gas,

spray voltage, capillary temperature, and aux gas heater temperature was 35 arbitrary units, 10 arbitrary units, 3500 V, 350 °C, and 300 °C, respectively. The obtained total ion chromatograms and MS fragments (m/z) were shown in Figs. S3 and S4, respectively.

Tables

Table S1 Calibration curve, linearity, linear regression coefficient (R^2), and limit of detection (LOD) for determination of carbamazepine, ciprofloxacin, and tetracycline by HPLC-UV method

Compound	Detection wavelength	Calibration curve	Linearity (ng/mL)	R^2	LOD (ng/mL)	RSD (%)
Carbamazepine	285 nm	y=18.287x+2292.7	5-1000	0.9992	2.34	1.89
Ciprofloxacin	275 nm	y=11.279x+2457.0	5-1000	0.9999	3.27	2.15
Tetracycline	355 nm	y=5.986x+1511.6	5-1000	0.9998	4.09	3.37

Note: The limit of detection (LOD) was evaluated on the basis of a signal-to-noise ratio of 3.

77 Table S2 Results of N_2 adsorption-desorption characteristics on the E-spun PANCMA

78 and g-C_3N_5/MIL-101(Fe)/PANCMA NFs

Property	Parameter	PANCMA	g-C_3N_5/MIL-101(Fe)/PANCMA
Surface Area	Single point surface area at P/Po (m^2/g)	24.9760	21.6322
	BET Surface Area (m^2/g)	25.8848	22.3689
	t-Plot External Surface Area (m^2/g)	26.1887	22.2204
	BJH Adsorption cumulative surface area of pores between 1.7000 nm and 300.0000 nm diameter (m^2/g)	25.036	21.673
	BJH Desorption cumulative surface area of pores between 1.7000 nm and 300.0000 nm diameter (m^2/g)	46.0199	45.4090
Pore Volume	Single point adsorption total pore volume of pores less than 130.9985 nm diameter at P/Po=0.985000000 (cm^3/g)	0.134838	0.091247
	t-Plot micropore volume (cm^3/g)	-0.000190	0.000056
	BJH Adsorption cumulative volume of pores between 1.7000 nm and 300.0000 nm width (cm^3/g)	0.138315	0.095571
	BJH Desorption cumulative volume of pores between 1.7000 nm and 300.0000 nm diameter (cm^3/g)	0.140227	0.097206
Pore Size	Adsorption average pore width (4V/A by BET) (nm)	20.83660	16.31683
	BJH Adsorption average pore width (4V/A) (nm)	22.0990	17.6388
	BJH Desorption average pore width (nm)	12.1884	8.5672

79

81

82 TableS 3 Comparison of the developed g-C_3N_5/MIL-101(Fe)/PANCMA nanofibers

83 with the other reported photocatalytical materials for removal of carbamazepine

84

Materials	Removal mode	Time (min)	Removal efficiency	Cycle times	Referencev
α-Fe_2O_3/MIL-101(Cr)	Photocatalytic degradation	180	100%	4	[42]
Bis-PDI-T@TiO_2	Photocatalytic degradation	30	95%	4	[43]
TiO_2/carbon dots/polyaniline	Photocatalytic degradation	60	77.63%-83.29%	5	[45]
Co_3O_4/$CuBi_2O_4$/SmVO_4	Photocatalytic degradation	300	76.1%	4	[46]
$AgIO_3$/$BiVO_4$	Photocatalytic degradation	60	97.86%	1	[47]
E-spun g-C_3N_5/MIL-101(Fe)/PANCMA nanofibers	Photocatalytic degradation	40	94.2%	15	This work

85

Figure S1 The appearance of g-C_3N_5/MIL-101(Fe) composites (A), E-spun PANCMA (B), and E-spun g-C_3N_5/MIL-101(Fe)/PANCMA (C) nanofibers

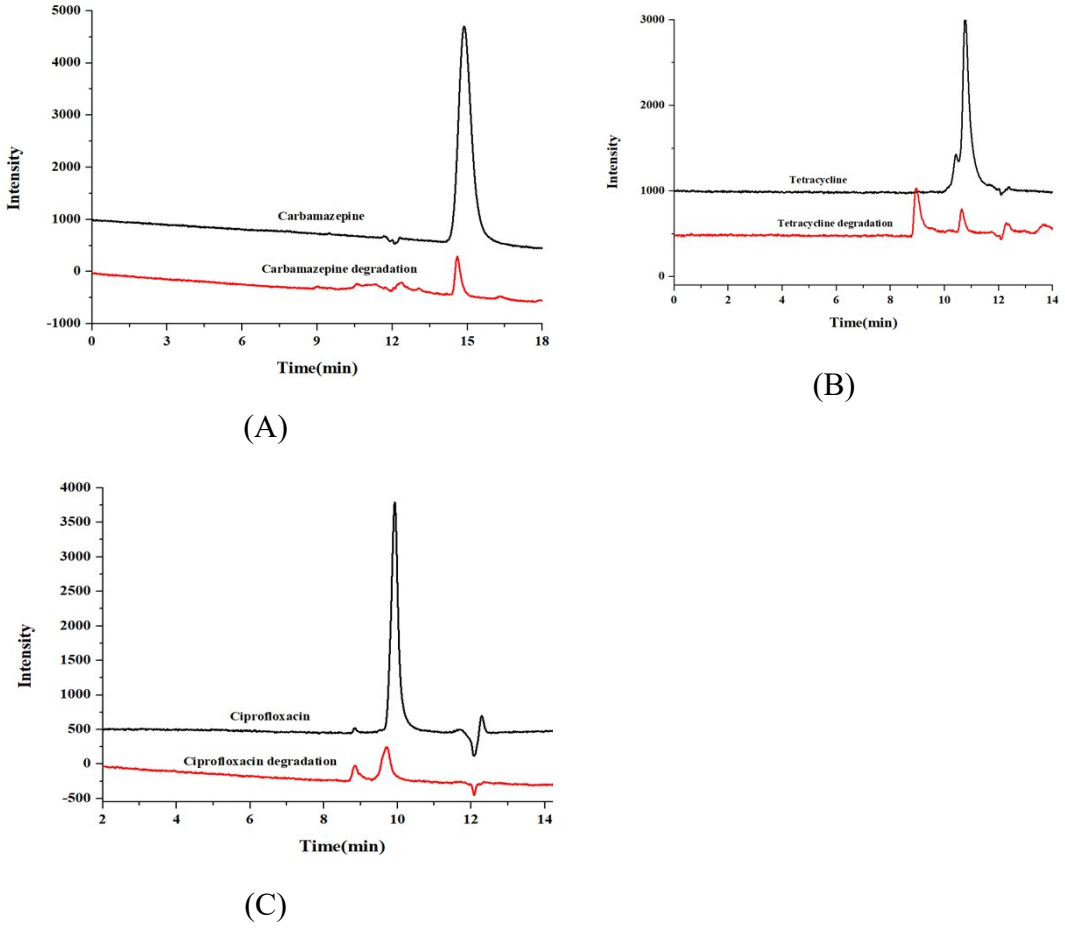

Figure S2 Typical HPLC-UV chromatograms of carbamazepine (A), tetracycline (B), and ciprofloxacin (C) before and after photocatalytical degradation with E-spun g-C_3N_5/MIL-101(Fe)/PANCMA NFs. The orignal concentration spiked in sample solution was 200 ng/mL.

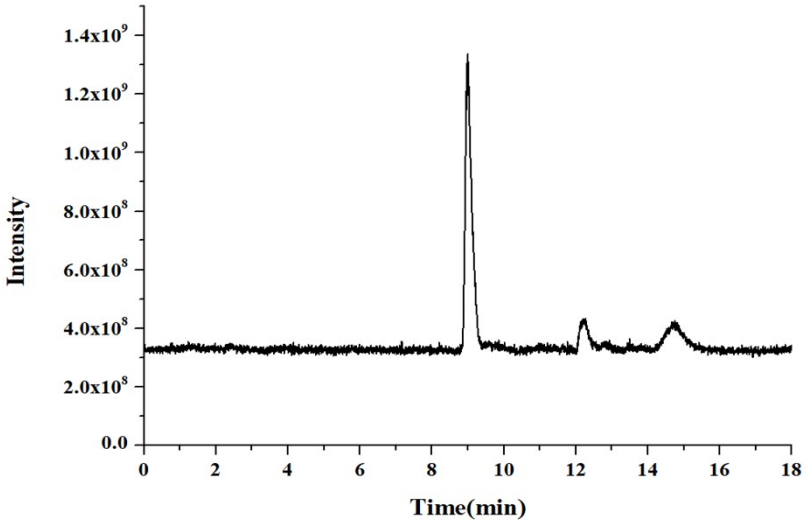

Figure S3 Typical total ion chromatograms of degradation products by photocatalytic degradation of carbamazepine with E-spun g-C_3N_5/MIL-101(Fe)/PANCMA nanofibers.

109

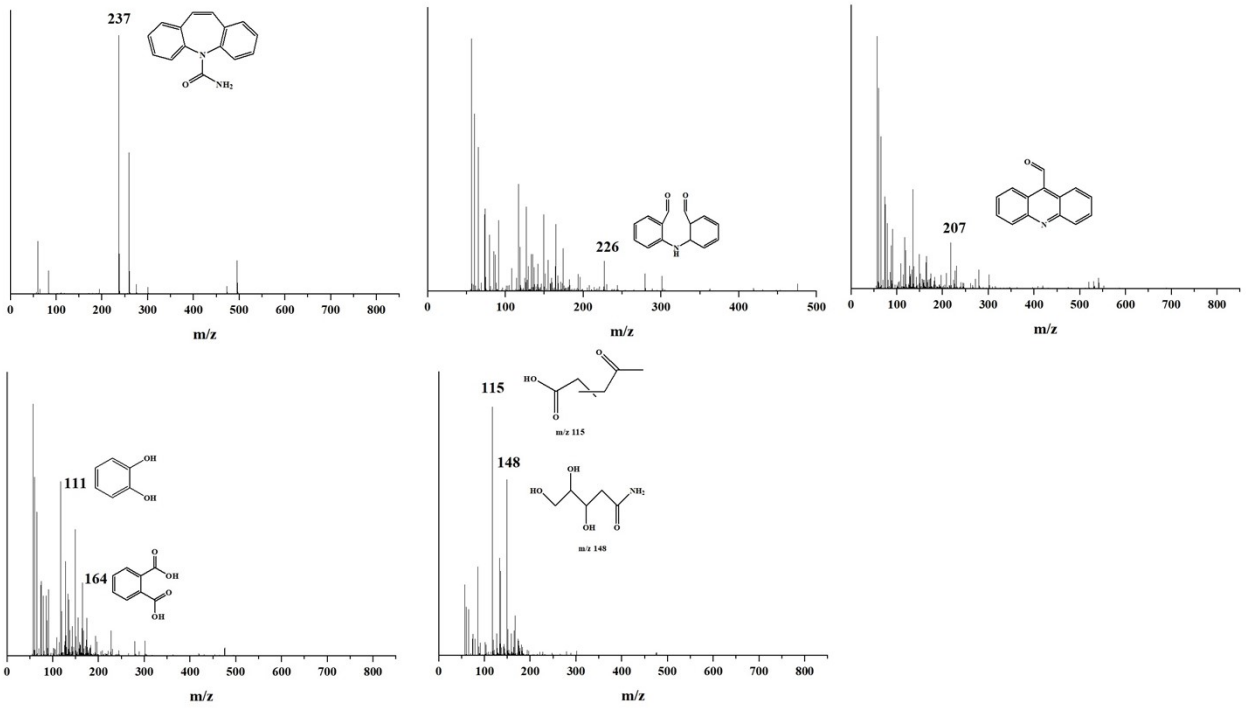

110

111 **Figure S4** Typical MS of photodegradation products obtained by LC-MS method.

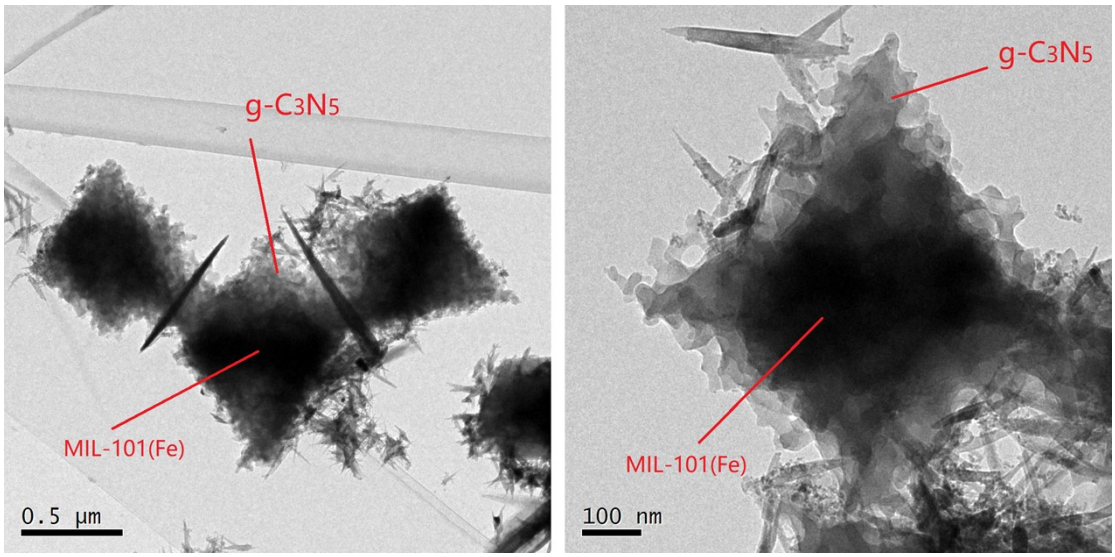

Figure S5 TEM images of g-C_3N_5/MIL-101(Fe) composites.

117

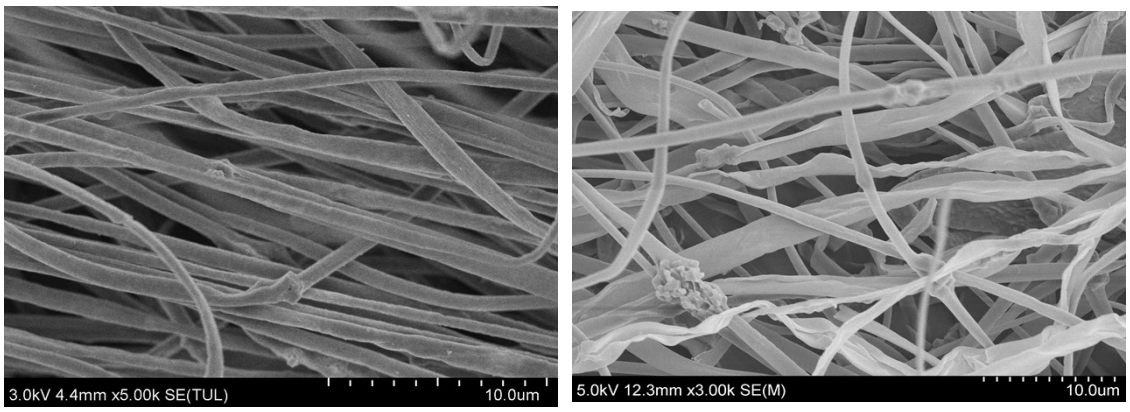

(A) (B)

118 **Figure S6** SEM images of E-spun g-C_3N_5/MIL-101(Fe)/PANCMA NFs before and

119 after consecutive 20 cycle times of photocatalytic degradation process.

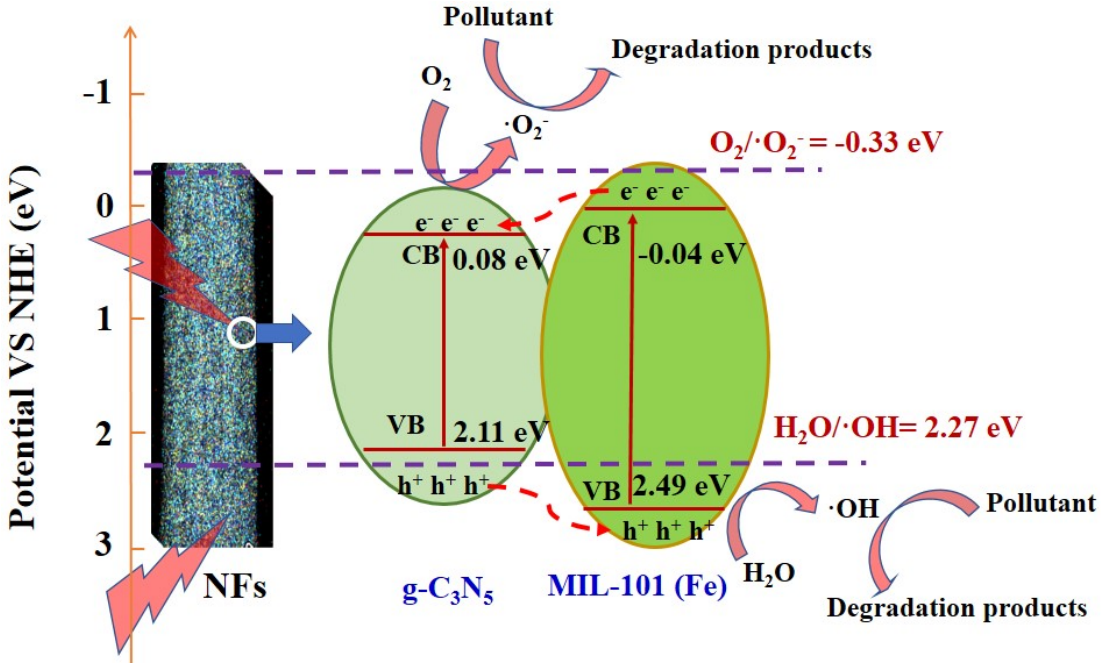

121

122 Figure S7 The possible degradation mechanism of g-C_3N_5/MIL-101(Fe)/PANCMA

123 towards carbamazepine pollutant.

124